SENSITIVITIES AND INTEGRATED AERODYNAMIC-STRUCTURAL OPTIMAL DESIGN

Giacomo Arsuffi
ENEA - Casaccia Research Center, Rome, Italy

Franco Mastroddi
Università di Roma "La Sapienza", Rome, Italy
and
Luigi Morino
Terza Università di Roma, Rome, Italy

Abstract

The objective of this research is to investigate the application of a new methodology based on a boundary element method to compute aerodynamic sensitivities to a simple integrated aerodynamic-structural optimal design problem. The selected problem was the design of a wing for minimum weight with structural-load, aeroelastic and performance constraints. An equivalent beam model was used to simulate the structure. The numerical results of this preliminary study show the validity of the proposed approach.

Introduction

In recent years there has been an increasing interest in integrated optimal design methods as a rational approach to the aircraft design problem (Sobieski [1]). In these methods, objective and constraint functions are assigned and the system analysis is performed by integrating several disciplines (*e.g.*, aerodynamics, structures, controls etc.) in a common optimization procedure. If a formal optimization is used, gradients of the objective and constraint functions with respect to the design variables of interest are required. This in turn implies the computation of the so-called sensitivities coefficients, *i.e.*, the derivatives with respect to the design variables of certain key quantities describing the system. In the field of computational structures, the subject of sensitivity analysis is relatively mature, and the references that are available are extensive (see, *e.g.*, references cited in Haftka and Gürdal [2]). In the field of aerodynamics, there exist a limited number of studies and research is actually in progress on this subject (Burgreen and Baysal [3]).
The present work is based on a methodology to compute aerodynamic sensitivities which is based on the Boundary Element Method (BEM) proposed by Morino [4]. In early works, Arsuffi [5] introduced these sensitivities to compute static aeroelastic sensitivities for a wing in the presence of shape design variable perturbations and Balis Crema et al. [6], performed a study to investigate aeroelastic sensitivities due to structural modification by using BEM aerodynamics.
In this paper the above methodologies are applied to solve an integrated aerodynamic-structural optimal design problem. The design problem of a wing for minimum weight in the presence of structural-load, aeroelastic, and performance constraints is addressed and solved. The objective is to investigate the aspects related to the integration of the proposed aerodynamics with a structural model in a common formal optimization scheme.
In the following sections the paper presents a description of the model used in the study and the formulation of the complete design problem. The optimization procedure used is described. Finally, initial numerical results are presented and discussed.

Modeling of the system

Aerodynamic analysis

For simplicity, in this paper the flow is assumed to be potential (except for a vector for a vortex layer called the wake, see Morino [7]), and incompressible (for the extension of the methodology to compressible and viscous flows see Morino [7]). The equation for the velocity potential, obtained from the continuity equation, is:

$$\nabla^2 \phi = 0 \qquad (1)$$

The boundary conditions, in the air frame of reference (*i.e.*, a reference frame fixed with the undisturbed air), are: (*i*) $\partial\phi/\partial n = \chi = \mathbf{n}\cdot\mathbf{v}_B$ on the body surface S_B (where $\mathbf{v}_B$ is the velocity of a point on the body surface and $\mathbf{n}$ the outward normal); (*ii*) $\phi = 0$ at infinity; (*iii*) potential discontinuity $\Delta\phi =$ constant following a material wake point; (*iv*) $\Delta(\partial\phi/\partial n) = 0$ on the wake surface S_W; (*v*) at the trailing edge, $\Delta\phi$ on the wake is equal to the potential discontinuity on the body.
The corresponding boundary integral representation is (Morino [7])

$$E_*\phi(\mathbf{x}_*,t_*) = \oiint_{S_B}\left(\frac{\partial\phi}{\partial n}G - \phi\frac{\partial G}{\partial n}\right)dS(\mathbf{x}) - \iint_{S_W}\Delta\phi\frac{\partial G}{\partial n}\,dS(\mathbf{x}) \qquad (2)$$

where $G = -1/4\pi\|\mathbf{x}-\mathbf{x}_*\|$, with $\mathbf{x}$ denoting the point of integration, whereas $E_* = 1$ if $\mathbf{x}_*$ is outside S_B, and $E_* = 1/2$ if $\mathbf{x}_*$ is a smooth point of S_B. In this last case Eq. 2 is an integral equation which allows one to solve for ϕ on S_B, given $\partial\phi/\partial n$ (from body boundary condition) and $\Delta\phi$ (from wake boundary condition). This equation is discretized by dividing S_B and S_W in quadrilateral elements (σ_m and σ'_n, respectively), assuming ϕ, χ, and $\Delta\phi$ to be constant within each element, and using the collocation method. Using M elements on S_B and N elements on S_W, one obtains (see, again, Morino [7]):

$$\sum_{m=1}^{M}\left(\frac{1}{2}\delta_{km} - C_{km} - \sum_{n=1}^{N}F_{kn}S_{nm}\right)\phi_m = \sum_{m=1}^{M}B_{km}\chi_m$$

($k = 1,\ldots,M$) where

$$B_{km} = \iint_{\sigma_m}G_k\,d\sigma(\mathbf{x}); \qquad C_{km} = -\iint_{\sigma_m}\frac{\partial G_k}{\partial n}\,d\sigma(\mathbf{x});$$
$$F_{kn} = -\iint_{\sigma'_n}\frac{\partial G_k}{\partial n}\,d\sigma(\mathbf{x})$$

with $G_k = -1/4\pi\|\mathbf{x}-\mathbf{x}_k\|$, whereas S_{nm} is equal to 1 if the m-th body surface element is the upper element at the trailing edge corresponding to the wake element n, equal to -1 for the lower element, zero otherwise, so that $\Delta\phi_n = \sum_m S_{nm}\phi_m$.
Next, consider the problem of computing lift and induced drag for a wing starting from the solution of Eq. 2, which gives the value of the velocity potential over the body surface S_B, and hence the value of the discontinuity of the potential along the trailing edge, $\Delta\phi_{TE}$. The lift is then obtained as:

$$L = \rho U_\infty\int_{-b/2}^{b/2}\Delta\phi_{TE}(y)\,dy \qquad (3)$$

where ρ is the air density, U_∞ the undisturbed flow velocity and b the wing span, whereas the induced drag can be computed with another line integral according to Trefftz approach (*e.g.*, see Ashley and Landhal [10]). Introducing the position coordinate ϑ such as $\cos\vartheta = -2y/b, 0 \le \vartheta \le \pi$ and approximating the velocity circulation $\Delta\phi_{TE}(y)$ – as evaluated by the Boundary Element Method – by a trigonometric expansion

$$\Delta\phi_{TE}(\vartheta) = U_\infty b\sum_{\substack{n=1\\ n\ odd}}^{N}A_n\sin n\vartheta \qquad (4)$$

(where the sum spans over the odd terms because a symmetric span distribution of the circulation is assumed), one obtains the following expression for the induced drag:

$$D_i = \frac{\pi\rho U_\infty^2 b^2}{8}\sum_{\substack{n=1\\ n\ odd}}^{N}nA_n^2 \qquad (5)$$

Structural analysis

The wing-like-box behaviour has been simulated by a beam model. The assumptions in this analysis was the following:

i -) beam cross sections with infinite stiffness in their plane and that give no contribution to the stiffness in normal direction;

ii -) skin panels working to shear stress only;

iii -) skin panel thickness small with respect to the cross section size;

iv -) spar and stringer cross section areas are considered as concentrated in one point for the evaluation of moment of inertia.

Moreover, in the present analysis all the geometrical properties are assumed to be constant along the span and over the section (*i.e.*, spar and stringer cross section areas, skin panel thickness, etc.).
The equilibrium equations, written in terms of displacements for the static case and negleting shear flexibility, are:

$$L_b w = \psi_b(y)$$
$$L_t\theta = \psi_t(y)$$

where w represents the vertical displacement of the elastic-center line and θ the rotation of the cross section, whereas $\psi_b(y)$ and $\psi_t(y)$ are distributed bending and torsional loads respectively, and the bending and the torsional operators are defined as:

$$L_b := \frac{\mathrm{d}^2}{\mathrm{d}y^2}EI\frac{\mathrm{d}^2}{\mathrm{d}y^2} \qquad L_t := -\frac{\mathrm{d}}{\mathrm{d}y}B\frac{\mathrm{d}}{\mathrm{d}y}$$

Boundary conditions for the problem are those of a cantilever beam with length $L = b/2$. For the bending problem they are:

$$\begin{cases} w(0) = w^I(0) = 0 \\ w^{II}(L) = w^{III}(L) = 0 \end{cases} \quad (6)$$

and for the torsion one:

$$\begin{cases} \theta(0) = 0 \\ \theta^I(L) = 0 \end{cases} \quad (7)$$

Solving the bending and the torsional problems by the eigenfunction method, displacements can be expressed as

$$w(y) = \sum_{n=1}^{\infty} w_n \phi_n^{(b)}(y) \quad (8)$$

and

$$\theta(y) = \sum_{n=1}^{\infty} \theta_n \phi_n^{(t)}(y) \quad (9)$$

being $\phi_n^{(b)}(y)$ and $\phi_n^{(t)}(y)$ bending and torsional problem eigenfunctions respectively.

Aeroelastic analysis

The aeroelastic problem (in the absence of structural damping), expressed in terms of Lagrangian variables $q_n(t)$ and natural modes of vibration $\boldsymbol{\phi}^n(\mathbf{x})$, is governed by the equation:

$$\frac{d^2\mathbf{q}}{dt^2} + \mathbf{\Lambda}^2\mathbf{q} = q\ \mathbf{e} \quad (10)$$

having denoted with $\mathbf{q}$ the Lagrangian coordinate vector, with $\mathbf{\Lambda}$ the diagonal matrix of the eigenvalues of the structure, with $q = \frac{1}{2}\rho_\infty U_\infty^2$ the dynamic pressure, and with $\mathbf{e}$ the vector of the generalized forces associated to the assumed modes $\boldsymbol{\phi}^n(\mathbf{x})$. Note that, assuming that the first M mode are of bending type ($\phi_n^{(b)}(y)$) and the other of torsional type ($\phi_n^{(t)}(y)$), one has

$$\boldsymbol{\phi}^n = \{\phi_n^{(b)}(y_1), \phi_n^{(b)}(y_2), ..., \phi_n^{(b)}(y_N)\}^T \quad \text{for } n \le M$$
$$\phi^n = \{\phi_{n-M}^{(t)}(y_1), \phi_{n-M}^{(t)}(y_2), ..., \phi_{n-M}^{(t)}(y_N)\}^T \text{for } n > M$$

being N is the number of points where the modes are evaluated and $\phi_n^{(b)}(y_i) = \phi_n^{(b)}(y)\Big|_{y=y_i}$. In this paper we examine only static aeroelastic constraints. Then, the Lagrangean variables do not depend by time so the Eq. 10 can be reduced to:

$$\mathbf{\Lambda}^2\mathbf{q} = q\ \mathbf{E}_s\mathbf{q} \quad (11)$$

where $\mathbf{E}_s$ is the so-called static portion of the aerodynamic matrix: indeed, the generalized aerodynamic forces can be expressed as

$$\mathbf{e} = \mathbf{E}\mathbf{q} \quad (12)$$

where $\mathbf{E}$ is the aerodynamic matrix derived by the BEM aerodynamic model (see App. B and Morino [11] for details on the aerodynamic matrix evaluation). The aerodynamic matrix is typically dependent on time or, in the Laplace domain, on the complex variable s. On the other hand, in the present study steady-state conditions have been considered, then the matrix $\mathbf{E}$ is independent of s and it will be referred as $\mathbf{E}_s$ in the following. The divergence dynamic pressure q_D is defined as the lower real value of q in correspondence of which the equation:

$$\left[\mathbf{\Lambda}^2 - q\mathbf{E}_s\right]\mathbf{q} = 0 \quad (13)$$

exhibits a trivial solution.

Performance

The mission profile considered in this study is described in the following: take-off, climbing, a cruise segment, descent and landing. The range is computed according to the Breguet equation:

$$R = \frac{v_c}{c}\frac{L}{D}\ln\frac{W_i}{W_f} \quad (14)$$

where v_c is the cruise speed, c the specific fuel consumption, L/D the lift to drag ratio, and W_i and W_f the initial and final weights of the cruise mission segment respectively. If the fuel consumptions in the mission segments before and during the cruise segment are expressed as a fraction of the usable mission fuel weight W_{uf} (indicated as k_1 e k_2 respectively), W_i e W_f can be written as:

$$W_i = W - k_1 W_{uf}; \qquad W_f = W - (k_1 + k_2)W_{uf} \quad (15)$$

Sensitivity analysis

The problem solution via formal optimization as in this study requires sensitivity computations to evaluate objective and constraint function derivatives according to the optimization algorithm requirements. Specifically, structural, aerodynamic and aeroelastic sensitivities are required in the present analysis.
Structural sensitivities, because of the equivalent-beam model chosen to describe the wing structure, can be expressed in analytical form. Derivatives of the bending moment at the wing root and those of the stiffness matrix with respect to the design variables are required. This also implies, the computation of the derivatives, with respect to the same variables, of the natural frequencies and natural modes of vibration of the structure. The bending moment at the wing root can be expressed as:

$$M_b = \frac{EI}{L^2}\frac{\partial^2 w}{\partial \eta^2} \quad (16)$$

in which $\eta = y/L$ denotes the wing span dimensionless abscissa ($L = b/2$), E Young's modulus, assumed constant for sake of semplicity, I the section moment of inertia, also constant, and $w(\eta)$ the bending deflection of the wing section of abscissa η. If α_i is the general design variable, the associated bending moment sensitivity is given by:

$$\frac{\partial M_b}{\partial \alpha_i} = \frac{E}{L^2}\left[\frac{dI}{d\alpha_i}\left(\frac{d^2w}{d\eta^2}\right) + I\frac{d}{d\alpha_i}\left(\frac{d^2w}{d\eta^2}\right)\right] + EI\left(\frac{d^2w}{d\eta^2}\right)\frac{d}{d\alpha_i}\left(\frac{1}{L^2}\right) \quad (17)$$

Further details are given in the App. A.
Next, consider aerodynamic (lift and induced drag) sensitivities. Lift sensitivity with respect to the design variable α_i, if the potential discontinuity sensitivity $\partial\Delta\phi_{TE}(y)/\partial\alpha_i$ is known (see App. B for details), can be obtained simply by differentiating Eq. 3:

$$\frac{\partial L}{\partial \alpha_i} = -\frac{\rho U_\infty}{2}\left(b\int_{-1}^{1}\frac{\partial\Delta\phi_{TE}(\eta)}{\partial\alpha_i}\,d\eta + \frac{\partial b}{\partial\alpha_i}\int_{-1}^{1}\Delta\phi_{TE}(\eta)\,d\eta\right) \quad (18)$$

where now $\eta = -2y/b$.
Similarly, by differentiating Eq. 5 the following relationship for the induced-drag sensitivity is obtained:

$$\frac{\partial D_i}{\partial \alpha_i} = \frac{\pi\rho U_\infty^2 b}{4}\left(\frac{\partial b}{\partial\alpha_i}\sum_{\substack{n=1\\ n\ odd}}^{N} nA_n^2 + b\sum_{\substack{n=1\\ n\ odd}}^{N} nA_n\frac{\partial A_n}{\partial\alpha_i}\right) \quad (19)$$

The derivatives $\partial A_n/\partial\alpha_i$ are related to $\partial\Delta\phi_{TE}(\vartheta)/\partial\alpha_i$ by the expression $\partial\Delta\phi_{TE}(\vartheta)/\partial\alpha_i = U_\infty[(\partial b/\partial\alpha_i)\sum^N A_n \sin n\vartheta + b\sum^N(\partial A_n/\partial\alpha_i)\sin n\vartheta]$ (obtained by differentiation of Eq. 4) and are computed by least-square fitting of the distribution $\partial\Delta\phi_{TE}(\vartheta)/\partial\alpha_i$ obtained by the solution of Eq. 38 in App. B.
Finally, let consider aeroelastic sensitivities, specifically divergence dynamic-pressure sensitivities. Starting from the Eq. 13, differentiating with respect to the design variable α_i, premultiplying by the transpose left eigenvector $\mathbf{v}^{(n)^T}$ of the eigenproblem associated to Eq. 13, and rearranging one has:

$$\frac{\partial q_D}{\partial\alpha} = \frac{1}{\mathbf{v}_D^T\mathbf{E}_s\mathbf{u}_D}\mathbf{v}_D^T\left[\frac{\partial\mathbf{\Lambda}}{\partial\alpha} - q_D\frac{\partial\mathbf{E}_s}{\partial\alpha}\right]\mathbf{u}_D \quad (20)$$

where details on the computation of derivatives of matrices $\mathbf{\Lambda}$ and $\mathbf{E}_s$ can be found in Apps. A and B respectively.

Integrated optimal design problem

The formulation introduced here has been applied to a simple integrated aerodynamic-structural optimal design problem. The goal of this study is to investigate the application of the aerodynamic sensitivities computed according to the proposed formulation to a simple multidisciplinary design problem. The selected problem is the integrated aerodynamic-structural design of a subsonic transport wing for minimum weight subject to required range and in presence of structural and aeroelastic constraints. The aspects of the optimization problem are detailed in the following sections.

Design variables, objective and constraint functions

The reference aircraft configuration is given in Tab. 1. The design variables considered are:

i) aspect ratio, $\alpha_1 = A$;

ii) wing surface, $\alpha_2 = S$;

iii) airfoil thickness at wing root section, $\alpha_3 = t_r$;

iv) airfoil thickness at wing tip section, $\alpha_4 = t_t$;

v) stringer cross-section area, $\alpha_5 = S_c$;

vi) wing-skin thickness, $\alpha_6 = t_h$;

vii) usable fuel weight for the mission, $\alpha_7 = W_{uf}$;

The objective function to be minimized is the gross weight of the aircraft W expressed as:

$$W = W_e + W_{uf} + W_p \quad (21)$$

where W_e is the aircraft standard empty weight and W_p the payload weight. The payload weight is assumed to be constant in the problem and equal to the reference configuration payload weight. W_{uf} is a design variable and changes as the optimization procedure progresses. The standard empty weight W_e is computed from the standard empty weight of the reference configuration, W_{re}, assuming that the reduction in the structural wing weight is reflected on the aircraft gross weight amplified by a factor η, due to corresponding savings in non structural weight and in the tail and fuselage:

$$W_e = W_{er} - \eta\,(W_{wr} - W_w) \quad (22)$$

where W_{wr} and W_w denote the actual and the reference structural wing weight respectively. A value $\eta = 2$ is assumend in the study.
The constraints assumed in this design problem are structural, aeroelastic and performance constraints. The imposed constraints are:

i) range R greater or equal to an allowable value, R_a;

ii) bending moment at the wing root M_a less or equal to an allowable value, M_{ba};

iii) divergence speed U_D greater or equal to an allowable value, U_{Da};

iv) wing volume available to contain fuel V_f greater or equal to the fuel volume required by the mission, V_{uf};

These constraint functions and their sensitivities are computed accordingly to the relationship that have been introduced in the previous sections. Regarding the limit values associated to these constraints, a maximum allowable bending moment of $M_{ba} = 450000kgm$ at the wing root has been assumed as structural strength constraint, while a minimum divergence speed of $U_{Da} = 180m/s$ has been required. Moreover, a minimum range value of $R_a = 2517km$ (1200 miles) has been imposed.

Optimization procedure

The described problem can be stated in terms of mathematical programming as follows:

$$\min_{\alpha} W(\alpha) \tag{23}$$

such that

$$g_1 = 1 - \frac{R}{R_a} \leq 0$$

$$g_2 = \frac{M_b}{M_{ba}} - 1 \leq 0$$

$$g_3 = 1 - \frac{U_D}{U_{Da}} \leq 0$$

$$g_4 = \frac{V_f}{V_{uf}} - 1 \leq 0$$

$$\alpha_i^l \leq \alpha_i \leq \alpha_i^u, \qquad i = 1, ..., 7$$

where α_i denote the design variables. The terms α_i^l and α_i^u indicate, respectively, the lower and the upper range limits for the design variable α_i.

To solve the above problem the Sequential Unconstrained Minimization Tecnique (SUMT, Fiacco and Mc Cormick [12]) with quadratic extended interior penalty function, Haftka and Gürdal [2], has been used. The sequence of unconstrained minimizations generated by this method have been resolved by the BFGS (*Broyden-Fletcher-Goldfarb-Shanno* , Gill et al. [13]) algorithm. The one-dimensional minimization associated to each search direction defined by the BFGS algorithm has been carried out by quadratic interpolation of the objective function.

Results and discussion

The initial design for optimization has been selected according to simple criteria based on the extrapolation of the aircraft characteristics similar to the small subsonic transport aircraft considered in the present analysis. Moreover, further semplifications have been introduced for sake of semplicity, accordingly to the objective of this work, an investigation on a methodology rather than to solve a detailed design problem. Accordingly, a rectangular planform wing has been considered, having a wing box with spars located at 0.1 and 0.8 of the chord, respectively, with twenty stringers, ten on the upper and ten on the lower sides of the wing box. The wing box hight has been assumed equal to 0.9 of the thickness of the section profile and wing-box skin thickness has assumed to be constant. The allowable value of the wing-root bending moment has been computed starting from the aircraft gross weight and the minimum divergence speed equals 1.2 the maximum cruise speed. The initial design configuration as well as the resulting final design are shown in Tab. 1. Using the above described optimization procedure the problem solution has been obtained in three unconstrained minimizations, each including four one-dimensional minimization procedures. The calculations have been performed on a DEC VAX 9000/440 system with a real CPU time approximately equal to two hours.

The gross weight convergence history is shown in Fig. 1. The gross weight of the aircraft has been reduced to $239kN$. This 10 percent reduction in weight compared with the reference aircraft is a consequence of the reduction in the wing and in the usable fuel weights.

The reduction in the wing structural weight is due to the inboard shift of the wing surface (resulting by the aspect ratio decrease, Fig. 2) which returns in a lower root bending moment, Fig. 3, and then in a wing size (Fig. 4) and weight (Fig. 5) reduction, because this effect is larger than the accompanying increase in induced drag. The wing weight decreases from $39kN$ to $29kN$, corresponding to a 25% weight saving.The empty weight reduction induced by this effect is partially responsable for the resulting usable fuel-weight saving.

The overall fuel weight reduction is of $6kN$, corresponding to a 15% fuel weight saving (Fig. 6). The reason for this reduction is, in addition to the above mentioned saving in wing structural weight, the initial 13% range excess with respect to the required value.

Finally, a special attention should be paid to the divergence speed time history. In fact, the initial configuration lies in the infeasible region of the design variable space because of the divergence speed constraint violation ($U_D = 154m/s$ instead of $U_D = 180m/s$). As the configuration changes in the optimization proce-

dure, the divergence speed increases to a final value of $181 m/s$, as shown in Fig. 7, which satisfies the divergence speed constraint.

Concluding remarks

A new methodology to compute aerodynamic sensitivities using a boundary element method has been applied to a simple integrated aerodynamic-structural optimal design problem. This study has shown the capability of the proposed metodology to deal with integrated aerodynamic-structural optimization problems taking into account the actual three-dimensional geometry of the wing. Numerical results indicate the validity and the accuracy of the metodology. The emphasys in this work was to investigate the application of the methodology to an integrated optimal design problem, so computational efficiency was not considered in detail, also if the analytical computation of the aerodynamic sensitivities is a significant contribution in this area. A complete evaluation of the computational requirements will be only possible after the optimization of the calculation procedure.

Acknowledgment

The authors gratefully acknowledge the contribution of Dr. S. Vigorito who was involved in the initial fase of this work.

References

1. Sobieszczanski-Sobieski, J., "Multidisciplinary Optimization for Engineering Systems: Achievements and Potential," DFVLR Symposium on Optimization, Bonn, Germany, 1989.
2. Haftka, R.T., Gurdal, E.Z., *Elements of Structural Optimization,* Kluwer, 1992.
3. Burgreen, G.W., and Baysal, O., "Aerodynamic Shape Optimization Using Preconditioned Conjugate Gradient Methods," AIAA Journal, Vol. 32, No. 11, 1994, pp. 2145-2152.
4. Morino, L., Chen, L. T., and Suciu, E. O., "Steady and Oscillatory Subsonic and Supersonic Aerodynamics Around Complex Configurations," AIAA Journal, Vol. 13, No. 3, 1975, pp. 368-374.
5. Arsuffi, G., "Metodo degli Elementi al Contorno per il Calcolo di Sensibiliterodinamiche con Applicazioni all'Ottimizzazione in Aeronautica," Tesi di Dottorato di Ricerca in Ingegneria Aerospaziale, Universitegli Studi di Roma "La Sapienza", Febbraio 1995.
6. Balis Crema, L., Mastroddi, F., Coppotelli, G., "Structural Modeling Effects on Aeroelastic Analysis," Proceedings of *International Forum on Aeroelasticity and Structural Dynamics,* Manchester, U.K., 26-28 June, 1995, Royal Aeronautical Society, pp. 40.1-40.11.
7. Morino, L., "Boundary Integral Equations in Aerodynamics," Applied Mechanics Reviews, Vol. 46, No. 8, 1993, pp. 445-466.
8. Mc Cullers, L.A., "Aircraft Configuration Optimization Including Optimized Flight Profiles," Proc. *Recent Experiences in Multidisciplinary Analysis and Optimization*, Hampton, Virginia, April 24-26, 1984.
9. Morino, L., Mastroddi, F., De Troia, R., Ghiringhelli, G. L., Mantegazza, P., "Matrix Fraction Approach for Finite-State Aerodynamic Modeling," *AIAA Journal,* Vol. 33, No. 4, April 1995, pp. 703-711.
10. Ashley, H., and Landhal, M., *Aerodynamics of Wing and Bodies* Addison-Wesley, 1965.
11. Morino, L., "Steady, Oscillatory, and Unsteady Subsonic and Supersonic Aerodynamics," Productions Version (SOUSSA-P 1.1) - Vol. 1, theoretical manual, NASA CR 159130, Jan. 1980.
12. Fiacco, A.V., and Mc Cormick, G.P., *Non Linear Programming: Sequential Unconstrained Minimization Tecniques,* John Wiley & Sons, N.Y., 1968.
13. Gill, P.E., Murray, W., and Wright, M.H., *Practical Optimization,* Academic Press, San Diego, 1981. N.Y., 1968.

Tab. 1 - Initial and Final Designs.

Objective function		
	Initial design	Final design
Gross weight, W	264.1 k N	238.5 k N

Design Variables		
	Initial design	Final design
aspect ratio, A	12.50	11.52
wing surface, S	45.34 m^2	38.97 m^2
wing root thickness, t_r	0.12	0.11
wing tip thickness, t_t	0.12	0.11
stringer cross-section area, A_c	3.000 cm^2	2.000 cm^2
cover-skin thickness, t_h	4.000 mm	2.500 mm
usable fuel weight, W_{uf}	40.00 kN	34.06 kN

Constraints		
	Initial design	Final design
range, R (R_a = 2220 km)	2517 km	2284 km
wing root bending moment, M_b (M_{ba} = 450 kNm)	262.1 kNm	207.7 kNm
divergence speed, U_D (U_{Da} = 180 m/s)	153.9 m/s	181.3 m/s
required (available) usable-fuel volume, V_{uf} (V_f)	4.347 m^3 (4.982 m^3)	3.018 m^3 (4.123 m^3)

Weights		
	Initial design	Final design
standard empty weight, W_e	164.1 kN	144.4 kN
structural wing weight, W_w	38.71 kN	28.87 kN
payload weight, W_p	60.00 kN	60.00 kN

Performance	
Cruise Mach number	0.50
Maximum operating Mach number	0.55
Cruise altitude	5500 m

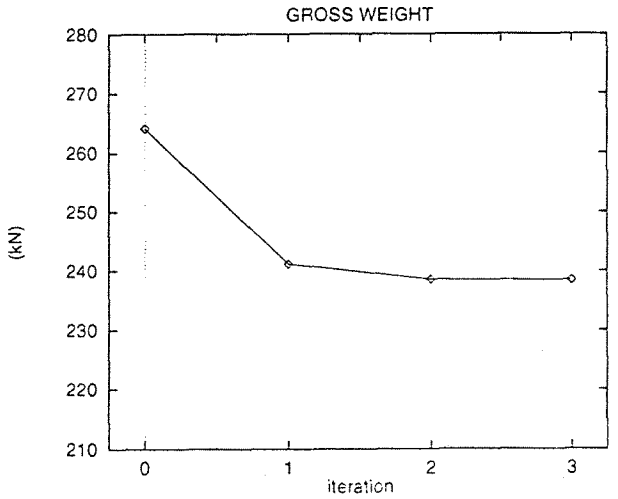

Figure 1: Convergence history of the gross weight, W.

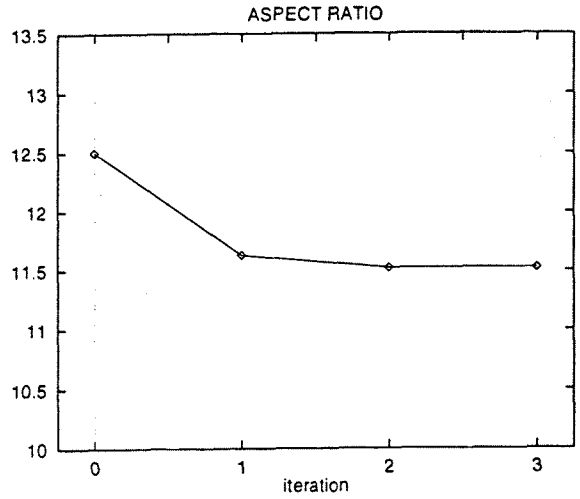

Figure 2: Convergence of the aspect ratio, A.

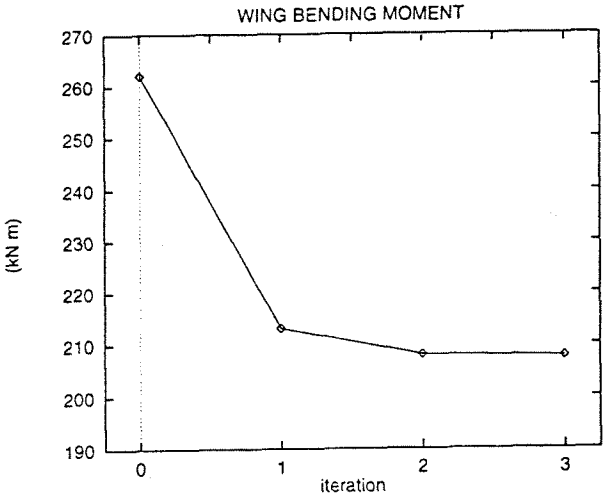

Figure 3: Convergence history of the wing-root bending moment, M_b.

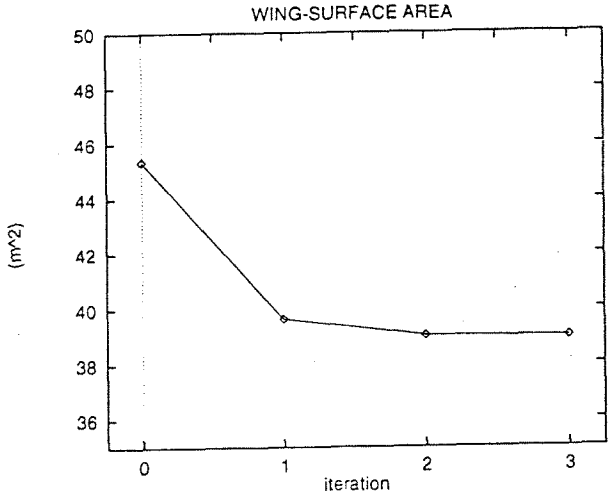

Figure 4: Convergence of the wing surface area, S.

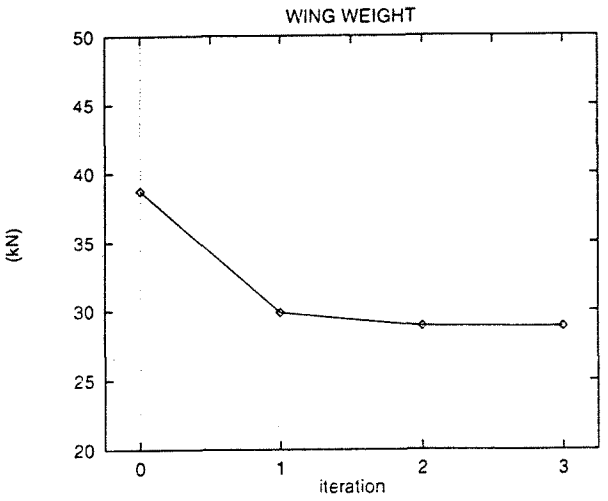

Figure 5: Convergence history of structural wing weight, W_w.

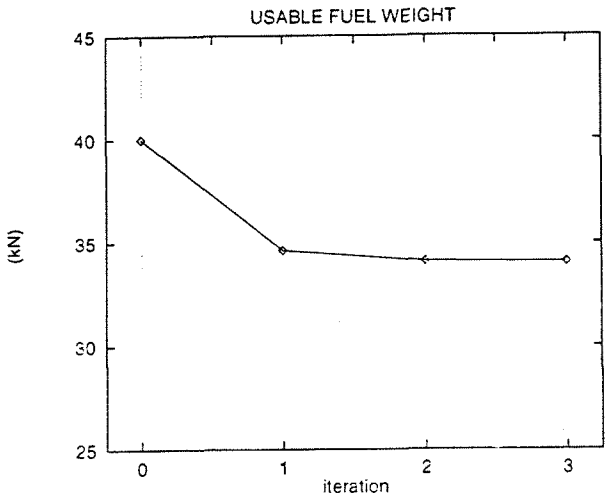

Figure 6: Convergence history of the usable fuel weight, W_{uf}.

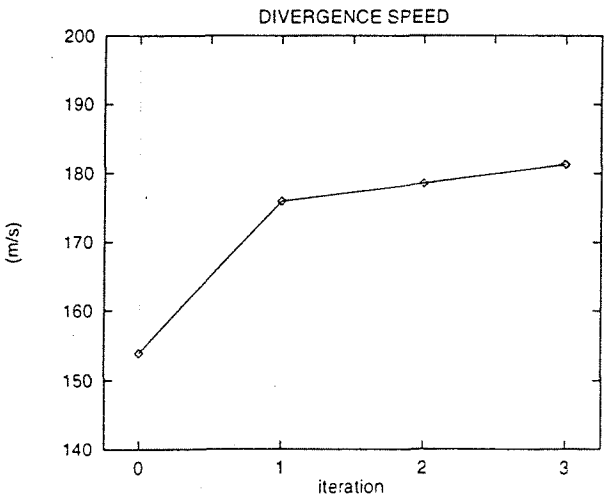

Figure 7: Convergence history of the divergence speed, V_D.

Appendix A

The natural modes of vibration for the equivalent beam can be expressed as

$$\phi_n^{(b)}(\eta) = c_{1n}^{(b)} \tilde{\phi}_n^{(b)}(\eta)$$

$$\phi_n^{(t)}(\eta) = c_{1n}^{(t)} \tilde{\phi}_n^{(t)}(\eta) \tag{24}$$

where $\eta = y/L$, and the normalization factors

$$\begin{aligned} c_{1n}^{(b)} &= \sqrt{\frac{1}{La_n}} \\ c_{1n}^{(t)} &= \sqrt{\frac{2}{L}} \end{aligned}$$

whereas

$$\begin{aligned} \tilde{\phi}_n^{(b)}(\eta) &= \Big[\cos(\mu_n^{(b)}\eta) - \cosh(\mu_n^{(b)}\eta) \\ &\quad + c_{2n}\left(\sin(\mu_n^{(b)}\eta) - \sinh(\mu_n^{(b)}\eta)\right)\Big] \\ \tilde{\phi}_n^{(t)}(\eta) &= \sin(\mu_n^{(t)}\eta) \end{aligned} \tag{25}$$

with

$$c_{2n} = -\frac{\cos\mu_n^{(b)} + \cosh\mu_n^{(b)}}{\sin\mu_n^{(b)} + \sinh\mu_n^{(b)}} \tag{26}$$

and $a_n = \int_0^1 \tilde{\phi}_n^{(b)^2}(\eta)\mathrm{d}\eta$. This last integral is solvable in closed form and $\mu_n^{(b)}$ and $\mu_n^{(t)}$ are obtained by the characteristic equation for the bending and torsional cantilever beam.

Note that the Equation 24 only the terms $c_{1n}^{(b)}$ and $c_{1n}^{(t)}$ depend upon the design variables chosen, so that the derivatives of the modes involve just these terms, that is

$$\begin{aligned} \frac{\partial c_{1n}^{(b)}(L)}{\partial A} &= \frac{-S}{4}\sqrt{\frac{2}{a}}(AS)^{-\frac{5}{4}} \\ \frac{\partial c_{1n}^{(b)}(L)}{\partial S} &= \frac{-A}{4}\sqrt{\frac{2}{a}}(AS)^{-\frac{5}{4}} \\ \frac{\partial c_{1n}^{(t)}(L)}{\partial A} &= \frac{-S}{2}(AS)^{-\frac{5}{4}} \\ \frac{\partial c_{1n}^{(t)}(L)}{\partial S} &= \frac{-A}{2}(AS)^{-\frac{5}{4}} \end{aligned} \tag{27}$$

where only non-zero derivatives with respect to the component of the design variables α_i (*i.e.*, aspect ratio and wing surface), are considered.

If the derivatives of the natural vibration modes are known, is possible to perform the computation of the derivatives of the bending moment at the wing root. In fact, starting form the definition

$$M_b = EI\frac{d^2w}{dy^2} \tag{28}$$

and considering the eigenfunction method, one can writes

$$w = \sum_{n=1}^{N} w_n \Phi_n^{(b)}(\eta) \qquad \text{with} \quad w_n = \frac{p_n}{\lambda_n} \tag{29}$$

having denoted with $p_n := \int_0^1 p\phi_n^{(b)}(\eta)d\eta$ the projection of the load p on the n-th mode $\Phi_n^{(b)}(\eta)$, and with λ_n the square of the $l'n$-th natural frequency.

Noting that in this case $\lambda_n = \mu_n^{(b)4}\frac{EI}{L^4}$, by substituting in Eq. 28 one obtains:

$$\begin{aligned} M_b &= \frac{EI}{L^2}\left[\sum_{n=1}^{N} c_{1n}^{(b)} \frac{p_n}{\mu_n^{(b)2}} \frac{L^4}{EI}\frac{d^2}{d\eta^2}\tilde{\phi}_n^{(b)}(\eta)\right] \\ &= L^2 \sum_{n=1}^{N} \frac{c_{1n}^{(b)} p_n}{\mu_n^{(b)2}} \tilde{\phi}_n^{(b)II}(\eta) \end{aligned} \tag{30}$$

and by differentiating

$$\frac{\partial M_b}{\partial A} = \sum_{n=1}^{N} \frac{p_n}{\mu_n^{(b)2}} \tilde{\phi}_n^{(b)II}(\eta) \frac{\partial (L^2 c_{1n}^{(b)})}{\partial A}$$

$$\frac{\partial M_b}{\partial S} = \sum_{n=1}^{N} \frac{p_n}{\mu_n^{(b)2}} \tilde{\phi}_n^{(b)II}(\eta) \frac{\partial (L^2 c_{1n}^{(b)})}{\partial S} \tag{31}$$

Indicating with $\tilde{c}_{1n}^{(b)}$ the term in the previous equations which depends upon the design variables, one obtains

$$\begin{aligned} \frac{\partial \tilde{c}_{1n}^{(b)}}{\partial A} &= \frac{3}{8}\sqrt{\frac{1}{2a}} S^{\frac{3}{4}} A^{-\frac{1}{4}} \\ \frac{\partial \tilde{c}_{1n}^{(b)}}{\partial S} &= \frac{3}{8}\sqrt{\frac{1}{2a}} A^{\frac{3}{4}} S^{-\frac{1}{4}} \end{aligned} \tag{32}$$

Next, consider the sensitivities of the stiffness matrix $\boldsymbol{\Lambda}$, that in this case is a diagonal matrix the elements of which are the squares of the natural frequency of the structure, that is

$$\lambda_n^{(b)} = \frac{EI}{L^4}\mu_n^{(b)4} \quad \lambda_n^{(t)} = \frac{B}{L^2}\mu_n^{(t)2} \tag{33}$$

for bending and torsional modes respectively. So in this case the sensitivities of the stiffness matrix are reduced to the computation of the sensitivities of the natural frequency of the structure.

The frequencies $\lambda_n^{(b)}$ depend upon the design variables by the area moment of inertia I and the length L. Similarly, the torsional frequencies $\lambda_n^{(t)}$ depend upon the design variable by Bredt's torsional stiffness B and the length L. Recalling that

$$\begin{aligned} I &= n_c\, A_c \left(\frac{d_c}{2}\right)^2 \\ B &= \frac{4G(d_c c_c)^2}{\beta} \\ \beta &= \frac{(2c_c + 2d_c)}{t_h} \end{aligned} \tag{34}$$

where n_c indicates the number of stringers, c_c denotes the wing-box chord, d_c the wing-box depth, E the Young's modulus and G the shear elasticity modulus, the frequencies can be expressed as function of the design variables, that is

$$\begin{aligned} \lambda_n^{(b)} &= \frac{16}{A^2 S^2} E n_c A_c \left(\frac{t_t + t_r}{2}\right)^2 \mu_n^{(b)4} \\ \lambda_n^{(t)} &= \frac{4G\mu_n^{(t)2} t_h k_c^2 (t_r + t_t)^2}{2A\sqrt{AS}k_c + A^2(t_r + t_t)} \end{aligned} \tag{35}$$

where the constants $\mu_n^{(b)4}$ and $\mu_n^{(t)2}$ are dependent on the the boundary conditions and the constant k_c is the wing-box to aerodynamic chord ratio. By differentiating bending frequencies one obtains

$$\begin{aligned} \frac{\partial \lambda_n^{(b)}}{\partial A} &= -\frac{2En_cA_c\,(t_t + t_r)^2}{A^3S^2}\mu_n^{(b)4} \\ \frac{\partial \lambda_n^{(b)}}{\partial A} &= -\frac{2En_cA_c\,(t_t + t_r)^2}{A^2S^3}\mu_n^{(b)4} \\ \frac{\partial \lambda_n^{(b)}}{\partial t_t} &= \frac{2En_cA_c\,(t_t + t_r)}{A^2S^2}\mu_n^{(b)4} \\ \frac{\partial \lambda_n^{(b)}}{\partial t_r} &= \frac{2En_cA_c\,(t_t + t_r)}{A^2S^2}\mu_n^{(b)4} \\ \frac{\partial \lambda_n^{(b)}}{\partial A_c} &= \frac{En_c\,(t_t + t_r)^2}{A^2S^2}\mu_n^{(b)4} \\ \frac{\partial \lambda_n^{(b)}}{\partial t_h} &= 0 \\ \frac{\partial \lambda_n^{(b)}}{\partial W_{uf}} &= 0 \end{aligned} \tag{36}$$

Furthermore, performing the same task for torsional frequencies yields

$$\frac{\partial \lambda_n^{(t)}}{\partial A} = -\frac{4G\mu_n^{(t)2} t_h k_c^2 (t_r + t_t)^2 \left[3\sqrt{AS}k_c + 2A(t_r + t_t)\right]}{\left[2A\sqrt{AS}k_c + A^2(t_r + t_t)\right]^2}$$

$$\frac{\partial \lambda_n^{(t)}}{\partial S} = -\frac{4G\mu_n^{(t)2} t_h k_c^2 (t_r + t_t)^2 \left[\frac{A^2}{\sqrt{AS}}k_c\right]}{\left[2A\sqrt{AS}k_c + A^2(t_r + t_t)\right]^2}$$

$$\frac{\partial \lambda_n^{(t)}}{\partial t_r} = \frac{\partial \lambda_n^{(t)}}{\partial t_t} = 4G\mu_n^{(t)2} t_h k_c^2 (t_r + t_t)$$

$$\left\{ \frac{2}{2A\sqrt{AS}k_c + A^2(t_r+t_t)} - \frac{A^2(t_r+t_t)}{\left[2A\sqrt{AS}k_c + A^2(t_r+t_t)\right]^2} \right\}$$

$$\frac{\partial \lambda_n^{(t)}}{\partial A_c} = 0$$

$$\frac{\partial \lambda_n^{(t)}}{\partial t_h} = \frac{4G\mu_n^{(t)2}k_c^2(t_r+t_t)^2}{2A\sqrt{AS}k_c + A^2(t_r+t_t)}$$

$$\frac{\partial \lambda_n^{(t)}}{\partial W_{uf}} = 0$$

Appendix B

The discretized boundary element intgral equation, Eq. 3, can be rewritten as:

$$\mathbf{Y}\boldsymbol{\phi} = \mathbf{b} \tag{37}$$

where $Y_{km} = \frac{1}{2}\delta_{km} - C_{km} - \sum_n F_{kn}S_{nm}$ and $b_k = \sum_m B_{km}\chi_m$. The derivative of the velocity potential with respect to the design variable α_i is:

$$\frac{\partial \boldsymbol{\phi}}{\partial \alpha_i} = \mathbf{Y}^{-1}\left[\frac{\partial \mathbf{b}}{\partial \alpha_i} - \frac{\partial \mathbf{Y}}{\partial \alpha_i}\boldsymbol{\phi}\right] \tag{38}$$

If the surface elements in which the body and wake surfaces are discretized are approximated by quadrilateral hyperboloidal elements (Morino et al., [4]), the terms B_{km}, C_{km} ed F_{kn} which appear in the elements of matrices $\mathbf{Y}$ e $\mathbf{b}$, Eq. 37, depend upon the location of the corners of the surface element m (or n) and of the collocation point $\mathbf{x}_k$, that is, the position vectors of five points, $\mathbf{x}^{(q)}$, which have components $x_l^{(q)}$, $l = 1,2,3$. Differentiating Eq. 37 and using the chain rule, yields:

$$\begin{aligned}\sum_{m=1}^{M} Y_{km}\frac{\partial \phi_m}{\partial \alpha_i} &= \sum_{m=1}^{M}\sum_{q=1}^{5}\sum_{l=1}^{3}\frac{\partial B_{km}}{\partial x_l^{(q)}}\frac{\partial x_l^{(q)}}{\partial \alpha_i}\chi_m \\ &+ \sum_{m=1}^{M} B_{km}\frac{\partial \chi_m}{\partial \alpha_i} \\ &- \sum_{m=1}^{M}\sum_{q=1}^{5}\sum_{l=1}^{3}\frac{\partial Y_{km}}{\partial x_l^{(q)}}\frac{\partial x_l^{(q)}}{\partial \alpha_i}\phi_m\end{aligned} \tag{39}$$

In a prescribed point of the design variable space $\boldsymbol{\alpha}$, Eq. 39 shows that the sensitivity computation can be performed by computing once, regardless the component α_i considered, both the matrix $\mathbf{Y}^{-1}$ as well as the terms $\partial Y_{km}/\partial x_l^{(q)}$ and $\partial B_{km}/\partial x_l^{(q)}$; these represent most of the computational effort involved. The terms $\partial \chi_m/\partial \alpha_i$ and $\partial x_l^{(q)}/\partial \alpha_i$, the only ones in Eq. 39 which depends on the design variable α_i, must be computed for each α_i, but their computation does not represent a problem, because simple expressions are available for them.

Consider the aerodynamic matrix $\mathbf{E}$ which relates the generalized aerodynamic forces $\mathbf{e}$ to the lagrangian variables $\mathbf{q}$:

$$\mathbf{e} = \mathbf{E}\mathbf{q} \tag{40}$$

It is convenient to decompose this matrix as follow (Ref. [11]):

$$\mathbf{E} = \mathbf{E}_4\left[\mathbf{E}_{3\phi}\mathbf{E}_2 + \mathbf{E}_{3\chi}\right]\mathbf{E}_1 \tag{41}$$

in which is possible to give a physical meaning to each term that appears in the right hand side, namely:

$$\begin{aligned}\boldsymbol{\chi} &= \mathbf{E}_1\mathbf{q} \\ \boldsymbol{\phi} &= \mathbf{E}_2\boldsymbol{\chi} \\ \mathbf{c}_p &= \mathbf{E}_{3\phi}\boldsymbol{\phi}_N + \mathbf{E}_{3\chi}\boldsymbol{\chi} \\ \mathbf{e} &= \mathbf{E}_4\mathbf{c}_p\end{aligned}$$

where $\boldsymbol{\chi}$ and $\mathbf{c}_p$ indicates the normalwash and the pressure coefficient vectors respectively and $\boldsymbol{\phi}_N$ the vector of the velocity potential ϕ computed at the nodes of the discretized body surface.
Now, considering the elements of the different matrices (see [11] for details). The elements of the vector $\mathbf{E}_{10}$ and of the matrix $\mathbf{E}_{11}$ are given by

$$E_{10k} = \mathbf{v}_B \cdot \mathbf{n}_{0k}$$

$$E_{11kj} = \mathbf{v}_B \cdot \Delta\mathbf{n}_{kj} \tag{42}$$

where $\mathbf{n}_0(\mathbf{x}_k) = \mathbf{n}_{0k}$ is the normal to the body surface corresponding to the control point $\mathbf{x}_k$ in the undeformed configuration and $\Delta\mathbf{n}_{kj}$ is the variation of the same vector in the deformed configuration associated to the j-th mode, *i.e.*,

$$\mathbf{n}(\mathbf{x}_k) = \mathbf{n}_{0k} + \sum_{j=1}^{N}\Delta\mathbf{n}_{kj}q_j \tag{43}$$

where

$$\begin{aligned}\mathbf{n}_{0k} &= \frac{\mathbf{a}_{1_0}(\mathbf{x}_k)\times\mathbf{a}_{2_0}(\mathbf{x}_k)}{|\mathbf{a}_{1_0}(\mathbf{x}_k)\times\mathbf{a}_{2_0}(\mathbf{x}_k)|} \\ \Delta\mathbf{n}_{kj} &= \frac{1}{|\mathbf{a}_{1_0}(\mathbf{x}_k)\times\mathbf{a}_{2_0}(\mathbf{x}_k)|}\left[\mathbf{a}_{1_0}(\mathbf{x}_k)\times\frac{\partial\boldsymbol{\Phi}_j(\mathbf{x}_k)}{\partial\xi_2}\right. \\ &\quad \left.+\mathbf{a}_{2_0}(\mathbf{x}_k)\times\frac{\partial\boldsymbol{\Phi}_j(\mathbf{x}_k)}{\partial\xi_1}\right]\end{aligned} \tag{44}$$

where $\mathbf{a}_{\alpha_0}$ and $\mathbf{a}_\alpha$ indicate the covariant base vector, in the undeformed and deformed configuration respectively, referred to the curvilinear coordinate system ξ^α. These covariant base vector are expressed by

$$\mathbf{a}_1(\mathbf{x}_k) = \frac{1}{4}\left(\mathbf{x}_{1m} + \mathbf{x}_{2m} - \mathbf{x}_{3m} - \mathbf{x}_{4m}\right)$$

$$\mathbf{a}_2(\mathbf{x}_k) = \frac{1}{4}\left(\mathbf{x}_{2m} - \mathbf{x}_{1m} + \mathbf{x}_{3m} - \mathbf{x}_{4m}\right) \qquad (45)$$

where $\mathbf{x}_{rm}$ indicates the position vector of the r-th node ($r = 1, 2, 3, 4$) of the surface element σ_m.
The elements of the matrix $\mathbf{E}_2$ are the form

$$E_{2km} = \sum_n Y_{kn}^{-1} B_{nm}$$

in which the matrices $\mathbf{Y}$ and $\mathbf{B}$ have been introduced earlier.
The matrices $\mathbf{E}_{3\phi}$ and $\mathbf{E}_{3\chi}$ are elements given by

$$\begin{aligned} E_{3\phi kr} &= -\frac{1}{2U_\infty}\left[S_{1r}\mathbf{a}_1(\mathbf{x}_k) + S_{2r}\mathbf{a}_2(\mathbf{x}_k)\right] \\ E_{3\chi km} &= -\frac{2}{U_\infty}\delta_{km}\,\mathbf{v}_R \cdot \mathbf{n} \end{aligned} \qquad (46)$$

where the index r denotes the r-th corner of the m-th surface element and the matrix S_{kr} is a trivial matrix which take into account for the right sign of the various terms.
Finally, the elements of the matrix $\mathbf{E}_4$ can be written as

$$E_{4jk} = -4\,q\,\mathbf{a}_1(\mathbf{x}_k) \times \mathbf{a}_2(\mathbf{x}_k)\,\boldsymbol{\Phi}_j(\mathbf{x}_k) \qquad (47)$$

Next, consider the derivatives of these matrices with respect to the design variable α_i. The derivatives of the elements of the vector $\mathbf{E}_{10}$ and of the matrix $\mathbf{E}_{11}$ are given by

$$\begin{aligned} \frac{\partial E_{10k}}{\partial \alpha_i} &= \mathbf{v}_R \cdot \frac{\partial \mathbf{n}_{0k}}{\partial \alpha_i} \\ \frac{\partial E_{11kj}}{\partial \alpha_i} &= \mathbf{v}_R \cdot \frac{\partial \Delta\mathbf{n}_{kj}}{\partial \alpha_i} \end{aligned} \qquad (48)$$

in which

$$\frac{\partial \mathbf{n}_{0k}}{\partial \alpha_i} = \sum_{r=1}^{4}\sum_{l=1}^{3} \frac{\partial \mathbf{n}_{0k}}{\partial x_{kr_l}} \cdot \frac{\partial x_{kr_l}}{\partial \alpha_i} \qquad (49)$$

By writing

$$\begin{aligned} \frac{\partial \mathbf{a}_1(\mathbf{x}_k)}{\partial \alpha_i} &= \frac{1}{4}\left(\frac{\partial \mathbf{x}_{1m}}{\partial \alpha_i} + \frac{\partial \mathbf{x}_{2m}}{\partial \alpha_i} - \frac{\partial \mathbf{x}_{3m}}{\partial \alpha_i} - \frac{\partial \mathbf{x}_{4m}}{\partial \alpha_i}\right) \\ \frac{\partial \mathbf{a}_2(\mathbf{x}_k)}{\partial \alpha_i} &= \frac{1}{4}\left(\frac{\partial \mathbf{x}_{2m}}{\partial \alpha_i} - \frac{\partial \mathbf{x}_{1m}}{\partial \alpha_i} + \frac{\partial \mathbf{x}_{3m}}{\partial \alpha_i} - \frac{\partial \mathbf{x}_{4m}}{\partial \alpha_i}\right) \end{aligned} \qquad (50)$$

yields

$$\begin{aligned} \frac{\partial \Delta\mathbf{n}_{kj}}{\partial \alpha_i} &= \left[\frac{\partial \mathbf{a}_1(\mathbf{x}_k)}{\partial \alpha_i} \times \frac{\partial \boldsymbol{\Phi}_j}{\partial \xi^2}\right] \\ &+ \left[\mathbf{a}_1(\mathbf{x}_k) \times \frac{\partial}{\partial \alpha_i}\left(\frac{\partial \boldsymbol{\Phi}_j}{\partial \xi^2}\right)\right] \\ &+ \left[\frac{\partial \mathbf{a}_2(\mathbf{x}_k)}{\partial \alpha_i} \times \frac{\partial \boldsymbol{\Phi}_j}{\partial \xi^1}\right] \\ &+ \left[\mathbf{a}_2(\mathbf{x}_k) \times \frac{\partial}{\partial \alpha_i}\left(\frac{\partial \boldsymbol{\Phi}_j}{\partial \xi^1}\right)\right] \end{aligned} \qquad (51)$$

Equation 51, using the relationship $\boldsymbol{\Phi}_j = c_{1j}(L)\tilde{\boldsymbol{\Phi}}_j$ and the Schwarz theorem may be written as

$$\begin{aligned} \frac{\partial \Delta\mathbf{n}_i}{\partial \alpha_i} &= \frac{\partial \mathbf{a}_1(\mathbf{x}_k)}{\partial \alpha_i} \times \frac{\partial \boldsymbol{\Phi}_j}{\partial \xi^2} + \frac{\partial \mathbf{a}_2(\mathbf{x}_k)}{\partial \alpha_i} \times \frac{\partial \boldsymbol{\Phi}_j}{\partial \xi^1} + \\ &\mathbf{a}_1(\mathbf{x}_k) \times \frac{\partial}{\partial \xi^2}\left(\tilde{\boldsymbol{\Phi}}_j \frac{\partial c_{1j}(L)}{\partial \alpha_i}\right) \\ &+\mathbf{a}_2(\mathbf{x}_k) \times \frac{\partial}{\partial \xi^1}\left(\tilde{\boldsymbol{\Phi}}_j \frac{\partial c_{1j}(L)}{\partial \alpha_i}\right) \end{aligned} \qquad (52)$$

in which all terms are known.
The derivatives of the matrix $\mathbf{E}_2$ involve the derivatives of the matrices $\mathbf{Y}$ and $\mathbf{B}$. This in turn implies the computation of the derivatives of the coefficients B_{km}, C_{km}, and F_{kn}, Eq. 3. The details are cumbersome and and can be found in Ref. [5].
By differentiating Eq. 46 with respect to α_i one obtains

$$\begin{aligned} \frac{\partial E_{3\phi kr}}{\partial \alpha_i} &= -\frac{1}{2U_\infty}\left[S_{1r}\frac{\partial \mathbf{a}_1(\mathbf{x}_k)}{\partial \alpha_i} + S_{2r}\frac{\partial \mathbf{a}_2(\mathbf{x}_k)}{\partial \alpha_i}\right] \\ \frac{\partial E_{3\chi km}}{\partial \alpha_i} &= -\frac{2}{U_\infty}\delta_{km}\,\mathbf{v}_R \cdot \frac{\partial \mathbf{n}}{\partial \alpha_i} \end{aligned} \qquad (53)$$

where derivatives of the covariant base vectors $\mathbf{a}_\alpha$ and of the normal $\mathbf{n}$ have been introduced above.
Starting from Eq. 47, using the notations introduced above yields

$$\begin{aligned} \frac{\partial E_{4_{jk}}}{\partial \alpha_i} &= -4\left(\frac{\partial \mathbf{a}_1(\mathbf{x}_k)}{\partial \alpha_i} \times \mathbf{a}_2(\mathbf{x}_k)\right. \\ &\left.+\mathbf{a}_1(\mathbf{x}_k) \times \frac{\partial \mathbf{a}_2(\mathbf{x}_k)}{\partial \alpha_i}\right)\boldsymbol{\Phi}_j \\ &-4\left(\mathbf{a}_1(\mathbf{x}_k) \times \mathbf{a}_2(\mathbf{x}_k)\right) \cdot \left(\tilde{\boldsymbol{\Phi}}_j \frac{\partial c_{1j}(L)}{\partial \alpha_i}\right) \end{aligned} \qquad (54)$$

in which all the terms have been already considered.